



Available online at www.sciencedirect.com



ScienceDirect

Trans. Nonferrous Met. Soc. China 30(2020) 1594–1604

Transactions of
Nonferrous Metals
Society of China

www.tnmsc.cn



Influence of additives and concentration of WC nanoparticles on properties of WC–Cu composite prepared by electroplating

Yu-chao ZHAO¹, Jian-cheng TANG¹, Nan YE¹, Wei-wei ZHOU¹, Chao-long WEI¹, Ding-jun LIU²

1. School of Materials Science and Engineering, Nanchang University, Nanchang 330031, China;

2. Institute for Advanced Study, Nanchang University, Nanchang 330031, China

Received 22 July 2019; accepted 7 May 2020

Abstract: The effects of additives (polyethylene glycol (PEG), sodium dodecyl sulfate (SDS)) and WC nano-powder on the microstructure, relative density, hardness and electrical conductivity of electroplated WC–Cu composite were investigated. The preparation mechanism was also studied. The microstructure of samples was analyzed by XRD, SEM, EDS, TEM and HRTEM. The synergistic effect of PEG and SDS made the WC–Cu composite more compact during the electroplating process. The hardness of WC–Cu composites increased with the increase in WC content, while the electrical conductivity decreased with the increase in WC content. The density of samples tended to increase initially and then decreased with increase in the additive content. When the electroplating solution contained 10 g/L WC nano-powder, 0.2 g/L PEG and 0.1 g/L SDS, the WC–Cu composite exhibited hardness of HV 221 and electric conductivity of 53.7 MS/m. Therefore, the results suggest that WC–Cu composite with excellent properties can be obtained by optimizing the content of additives and WC particles.

Key words: WC–Cu composite; electroplating; additives; microstructure; properties

1 Introduction

WC–Cu composites are functional materials with excellent comprehensive properties, which have attracted the attention of many researchers. WC has the advantages of high melting point, high hardness and good stability, and can be used as the contact material of refractory skeleton and the hard phase of wear-resistant material [1,2]. In addition, WC and Cu can be combined to form WC–Cu composite with good electrical and thermal conductivity, high wear resistance, high hardness and high-temperature softening resistance [3]. WC–Cu composites have broad prospective applications in integrated circuit (IC) lead frames, resistive welding electrodes, contact materials, commutators, etc [4–6].

At present, the common preparation methods

for WC–Cu composites include powder metallurgy, composite casting, mechanical alloying and hot pressing [7–11]. Powder metallurgy is a technology that uses mixed powders of WC and Cu as raw materials to form metal materials after forming and sintering. Sintering process has high requirements on equipment and high cost. Composite coating technology is a kind of surface engineering technology on the surface of the substrate, and then another surface engineering technology treatment is carried out to improve the surface state and performance of the material. However, the compactness and uniformity of the composite are poor. Mechanical alloying and hot-press sintering methods are simple, but they require long processing time and are expensive. Moreover, it is very difficult to obtain high density materials because WC and Cu do not dissolve in each other and WC particles hinder sintering.

Corresponding author: Jian-cheng TANG; Tel: +86-791-83969559; E-mail: tangjiancheng@ncu.edu.cn
DOI: 10.1016/S1003-6326(20)65322-5

Electroplating is an economical method for preparing nano-composite coatings in one step without secondary operations. During the plating process, high temperature, vacuum formation or expensive equipment are not required. Electroplating technology has become one of the well-researched methods in recent years due to its advantages such as simple process, low temperature, low cost, and ability to prepare coatings with low porosity and high density [12–15]. In nano-composite coating materials, the decrease in diameter of the reinforcing particles leads to substantial increase in hardness, strength, wear resistance and corrosion resistance of the coating. Such coating materials with enhanced properties are widely used in many industries including military industry. The commonly used reinforcing particles include SiO_2 , TiO_2 , Al_2O_3 , WC, SiC, AlN, graphite, carbon nanotubes, etc. [16–18]. In the process of electroplating, the nanoparticles at the grain boundary can prevent the movement of dislocations and recrystallization at high temperatures, which improves the microhardness and thermal stability [19]. ZHOU et al [20] reported a method for preparing Ni/WC/W₂S composite coatings on low carbon steel substrates through one-step electroplating, and successfully obtained nickel-based superhydrophobic coatings. AKBULUT et al [21] prepared Cu/WC/graphene nano-composites by electrophoretic deposition and investigated the effects of WC and graphene reinforcements on the structural and tribological properties of the Cu matrix. Cu/graphene coating and Cu/WC/graphene coating showed good wear performance under dry sliding condition. As the nanocomposite improves the load-carrying and self-lubricating properties of the material, the nanocomposite material has a lower coefficient of friction compared to pure copper plating [22]. However, most of the WC–Cu composite prepared by electroplating are powdery, and further sintering is needed to obtain compact alloy materials.

In this work, bulk WC–Cu composite was prepared by pulsed current (PC) electroplating by adjusting the content of additives (polyethylene glycol (PEG), sodium dodecyl sulfate (SDS)) and WC nano-powder. The effects of additives and WC nano-powder on the microstructure and properties including the relative density, microhardness and electrical conductivity of the samples were

investigated, and the preparation mechanism was elucidated.

2 Experimental

2.1 Pre-modified WC powders

In this experiment, WC nano-powder developed by our group was used as the reinforcing material [23]. Ammonium metatungstate and water-soluble organic carbon source were used as raw materials, and spray drying was carried out after full dissolution of raw materials in water. Then, WC nano-powder with an average particle size of 200 nm was prepared by continuous carbon–hydrogen coreduction–carbonization in a tube furnace and followed by ball milling. WC nano-powder was quickly mixed with PEG in de-ionized water. PEG is inexpensive and is commonly used as a dispersant to reduce powder agglomeration. PEG is also used as a suppressor or inhibitor which can reduce the deposition rate of copper by two orders of magnitude during electroplating [24,25]. The contents of WC powder and PEG accounted for 5 wt.% and 0.1 wt.%, respectively. The mixture was rapidly milled for 4 h in an agate grinding cylinder with agate ball at 800 r/min. After pretreatment, the mixture of WC powder and PEG was made into a suspension with water, which was then poured into a plating solution containing copper ions and mixed well.

2.2 Surface treatment of substrates

A copper plate with a purity of 99.999% was used as the cathode and anode. In order to minimize the effect of anodic polarization, the area ratio of the anode to the cathode was set to be 2:1 [26]. Before electroplating, copper plates were subjected to mechanical grinding from a low to high step using 1000 to 3000 grade silicon carbide sandpaper. Copper plates were then activated by submerging them in 5 vol.% sulfuric acid and then 10 vol.% hydrochloric acid for 2 min. Then, the plates were rinsed in running distilled water and finally dried in a forced air oven. The SEM micrograph of the processed copper plate is shown in Fig. 1.

2.3 Electroplating

Electroplating was performed using a two-electrode battery device, as shown in Fig. 2. The Plating Electronics (Yue Yang Electric Appliance,

60V/20A) pulse rectifier was used as the PC supply to provide a plating current density of 2 A/dm². The frequency and duty cycle were 1000 HZ and 40%, respectively. The process of electroplating was terminated at 10 h.

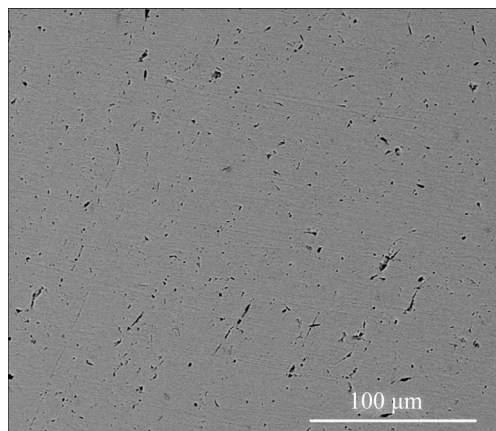


Fig. 1 SEM micrograph of processed copper plate

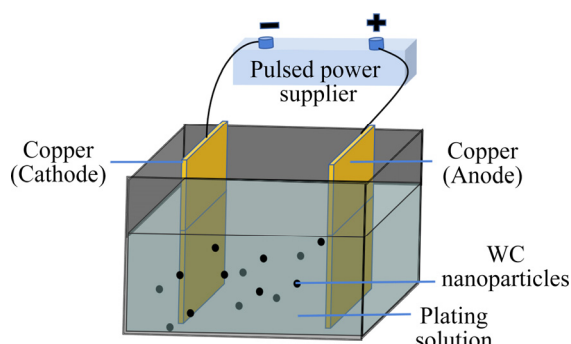


Fig. 2 Schematic of electroplating device for preparation of WC–Cu composites

The base electrolyte included 125 g/L CuSO₄·5H₂O, 200 g/L H₂SO₄ and 60 mg/L NaCl dissolved in 500 mL deionized water. With SDS as an accelerator, and PEG-4000 as a suppressor, the pre-modified WC powder were added with different concentrations (Table 1) to evaluate the effects of WC concentration on the morphology and properties of WC–Cu composites. In Samples 1, 2 and 3, the contents of PEG and SDS were 0.1 and 0 g/L, 0.1 and 0.1 g/L, and 0.2 and 0.1 g/L, respectively. In Samples 4 and 5, the contents of WC nano-powder were 10 g/L and 15 g/L, respectively. Except for the above variables, the content of other substances was the same.

In order to enhance the dispersibility of the WC particles, the solution was stirred with a magnetic stirrer during the electroplating process.

The plated WC–Cu composite was gently rinsed with absolute ethanol and dried in an oven at 60 °C.

Table 1 Chemical composition of electroplating bath (g/L)

Bath No.	CuSO ₄ ·5H ₂ O	H ₂ SO ₄	NaCl	PEG	SDS	WC powder
1	125	200	0.06	0.1	0	5
2	125	200	0.06	0.1	0.1	5
3	125	200	0.06	0.2	0.1	5
4	125	200	0.06	0.2	0.1	10
5	125	200	0.06	0.2	0.1	15

2.4 Characterization

Environmental scanning electron microscopy (SEM, FEI Quanta 200F) was used to evaluate the morphology of samples. X-ray diffraction (XRD, Bruker D8 X-ray diffractometer Focus) with Cu K_α radiation (40 kV and 40 mA) was used for phase analysis. High-resolution transmission electron microscopy (HR-TEM, FEI TalosF200X) was used to characterize the transition layer. The hardness was measured using a Micro-Vivtorinox hardness tester (HVS-1000). The electrical conductivity of composites was examined by digital conductivity instrument (Sigma 2008A). The densities of samples were measured using the Archimedes method. The content of W was measured by ICAP-6300 inductively coupled plasma spectrometer (ICP, Thermoelectric Company, USA).

3 Results and discussion

3.1 Characterization of pre-modified WC powder

SEM images of WC powders before and after pretreatment are shown in Figs. 3(a) and (b), respectively. As seen from Fig. 3(b), there was PEG coating on the surface of polygonal WC particles and the agglomeration of WC particles was also significantly reduced. Since the surface deposition activity of the WC powder is low, the coating on the electrode would not be uniform without surface pretreatment of the particles. Appropriate pretreatment of WC powders can not only improve the specific surface area of WC particles, but also enhance the adsorption, nucleation and growth ability of Cu on WC surface [27].

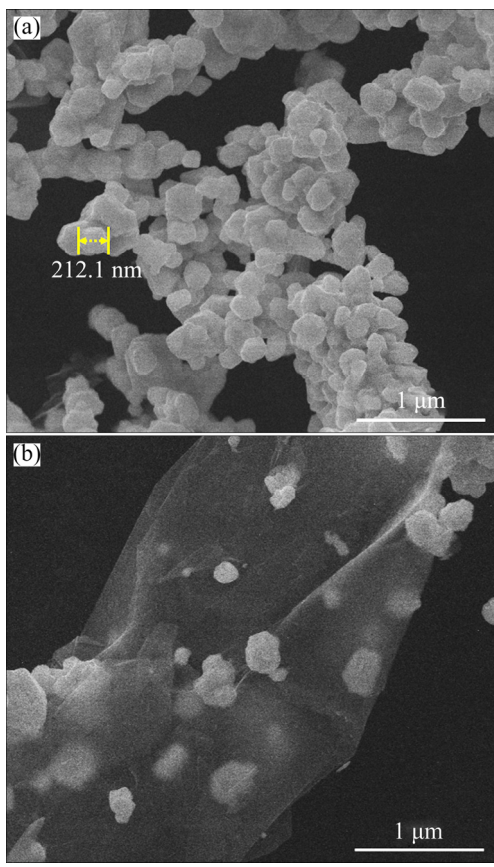


Fig. 3 SEM images of WC powder: (a) Untreated; (b) Treated

3.2 Microstructure of plating composite

Figure 4 shows XRD patterns of WC–Cu composites prepared using electroplating with different plating baths as well as the standard XRD patterns of Cu and WC. As seen in Fig. 4(a), WC–Cu composites only consisted of WC and Cu phases. The peaks at $2\theta=43.316^\circ$, 50.448° and 74.125° corresponded to the crystal planes of (111), (200) and (220), respectively, indicating the face-centred cubic structure of copper (Fig. 4(b)). The XRD results suggested that the copper ions were completely reduced to metallic copper. Three main low-intensity peaks were observed at $2\theta=31.512^\circ$, 35.642° and 48.297° , which corresponded to the (001), (100) and (101) crystal planes of WC, respectively (Fig. 4(c)). The WC peak intensity was the largest in the composite prepared by using plating Bath 5 (15 g/L WC). Therefore, the presence of WC peaks in the diffraction pattern confirmed that the WC–Cu composite was prepared by electroplating.

The cross-sectional SEM micrographs of the samples electroplated with different concentrations

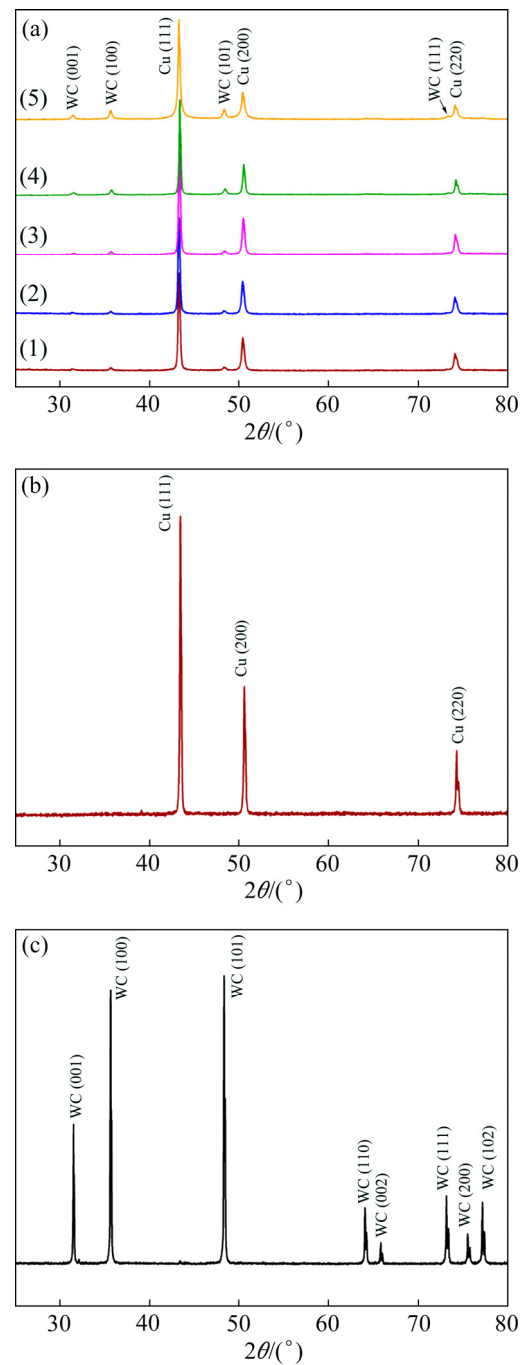


Fig. 4 XRD patterns of products (a) and standard XRD patterns of Cu (b) and WC (c)

of WC and additives are presented in Fig. 5. Figures 5(a), (b) and (c) correspond to the micrographs of Sample 1, Sample 2 and Sample 3, which were prepared in Bath 1, Bath 2 and Bath 3, respectively. As listed in Table 2, the content of WC nanoparticles in these three baths was the same, but the content of additives was varied. In Bath 2, 0.1 g/L SDS additive was present and in Bath 3, the content of PEG was increased to 0.2 g/L. By comparing the micrographs of the samples in

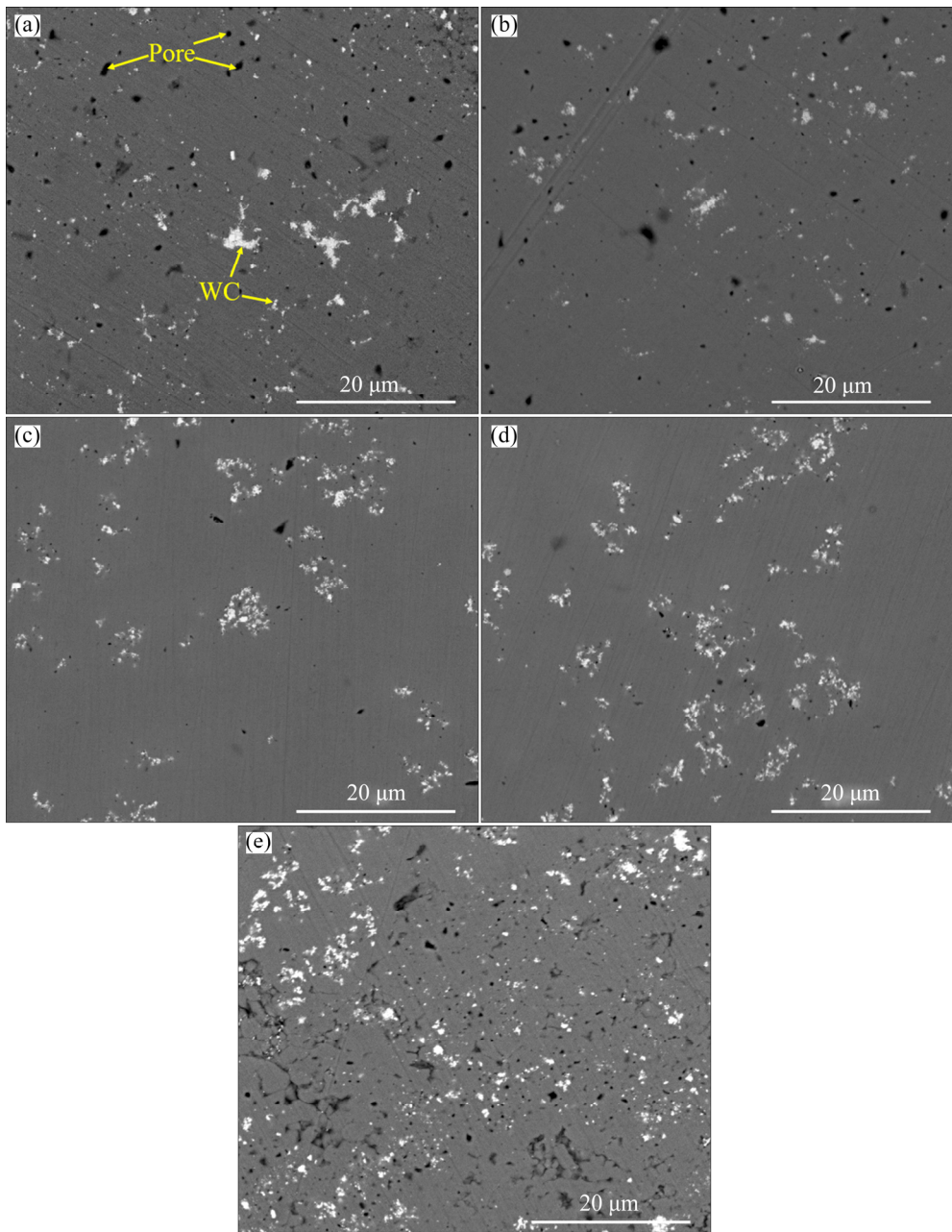


Fig. 5 Cross-sectional SEM micrographs of samples electroplated with different concentrations of WC and additives: (a) Sample 1; (b) Sample 2; (c) Sample 3; (d) Sample 4; (e) Sample 5

Figs. 5(a), (b) and (c), it can be seen that the difference in additives led to different morphologies. The pores in Samples 2 and 3 were significantly reduced and the copper matrix formed by electroplating was more compact. Additives in the plating bath have an important influence on the preparation of homogeneous plating materials. The formation mechanism of the dense plating material is driven by the competitive adsorption of the additive and the metal ion. The nucleation rate is accelerated by increasing the number of active sites so that the fine crystal alloy plating can be

produced [28].

Figures 5(d) and (e) correspond to the micrographs of Sample 4 and Sample 5, which were prepared in Bath 4 and Bath 5, respectively. The content of additives in both baths was the same, but the contents of WC nanoparticles in the two baths were 10 and 15 g/L, respectively. Compared to the micrograph of Sample 3, it can be seen that WC content in Cu matrix increased significantly for Sample 4 with the increase in WC content in electrolyte solution. This result was consistent with the XRD results. The increase in WC content in

electrolyte solution possibly led to an increase in the amount of WC particles adsorbed on the cathode surface. Furthermore, ICP was used to measure the content of W in the samples, and the WC content of the five samples was found to be 15.9, 15.7, 16.1, 27.3 and 36.2 wt.%, respectively. However, massive pores were observed in Sample 5 (Fig. 5(e)), most likely due to the presence of a large number of WC particles that blocked the electrodeposition of copper ions. The porosity was also influenced by gravity and mechanical agitation, along with the flow and shedding of a large number of tungsten carbide particles which increased the

formation of pores. Therefore, the physical performance of the electroplating composite was affected.

Figure 6 presents the SEM micrographs and EDS mapping results of the electroplated Sample 5. These results confirmed that WC was successfully plated and dispersed uniformly in the Cu matrix. The amount of the WC plated into the WC–Cu composite measured by EDS method was about 35.8 wt.%, which was similar to the results of ICP.

Additionally, particle distribution in WC–Cu composites was further determined by TEM analysis near the WC–Cu interface, as illustrated in

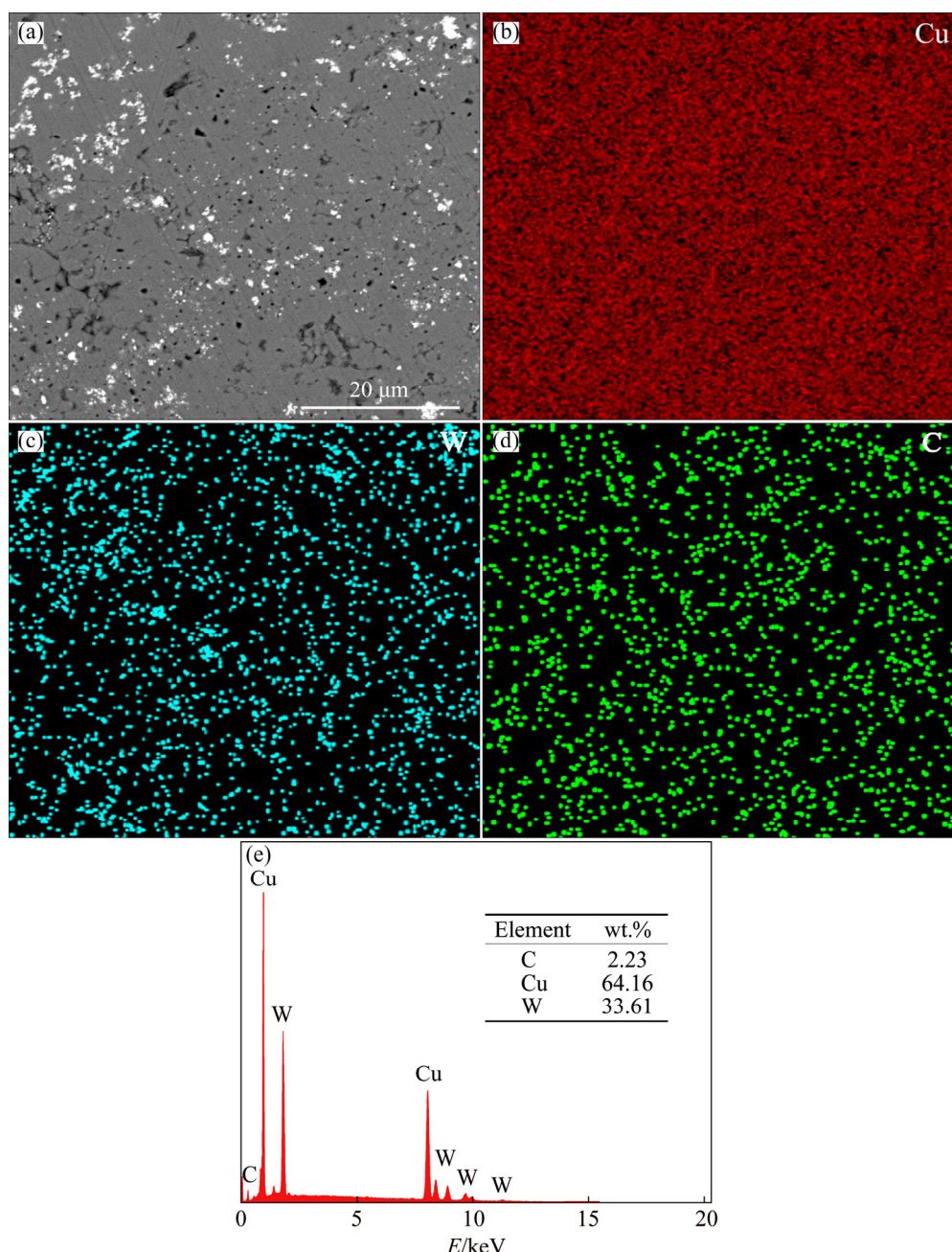


Fig. 6 SEM micrograph and EDS mapping results of electroplated Sample 5

Fig. 7. Grain boundaries were clearly observed in Fig. 7(a), and WC nanoparticles were uniformly dispersed around the grain boundaries. The WC–Cu interfaces consisted of WC (Position *d* and SAED

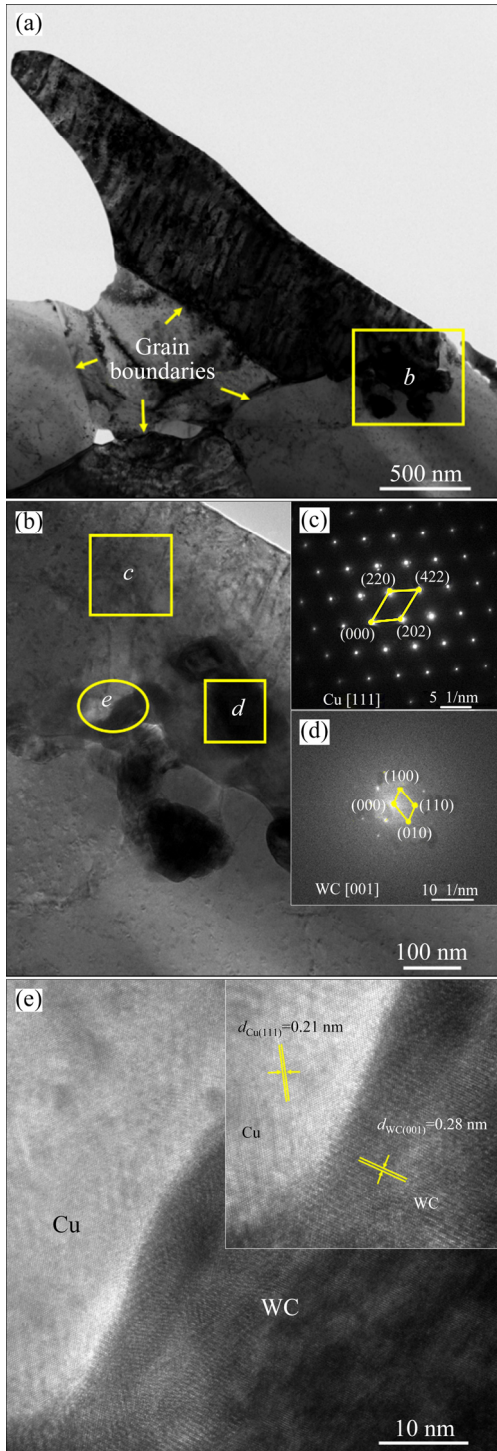


Fig. 7 TEM images of WC–Cu composite: (a) TEM image of Sample 4; (b) High magnification image of Position *b* in Fig. 7(a); (c) Electron diffraction pattern of Position *c* in Fig. 7(b); (d) Electron diffraction pattern of Position *d* in Fig. 7(b); (e) HR-TEM image of Position *e* in Fig. 7(b)

in Fig. 7(d)) embedded in Cu matrix (Position *c* and SAED in Fig. 7(c)). Figure 7(e) shows the HR-TEM image of the Position *e* in Fig. 7(b). As shown in the high-resolution image, the lattice fringe spacing in the light-colored region was 0.21 nm, which corresponded to the Cu (111) crystal plane. The lattice spacing of the dark areas was 0.28 nm, which was consistent with the WC (001) crystal plane. The orientation relationship of WC and Cu facilitated the strong bonding of the interface between the strengthened WC phase and the Cu matrix.

SEM images of the sample surfaces are shown in Fig. 8. The unpolished sample surface consisted of protrusions, similar to spherical, nodular structures and the sample was gradually densified. It has been reported that nodules originate from existing protrusion points, and the nodules appear to be spherical due to the minimization of surface energy during formation [29]. In the process of electroplating, WC nanoparticles were adsorbed on the cathode surface, providing the protrusion point. Cu ions (Cu^{2+}) were reduced to Cu around WC nanoparticles to form spherical composite.

The schematic diagram describing the formation of WC–Cu composites by electroplating is presented in Fig. 9. After pretreatment, PEG was wrapped around WC nanoparticles. When WC nano-powder was added to the electroplating bath, the nanoparticles dispersed in the electroplating solution and were simultaneously encapsulated by SDS and Cl^- . When the pulse power was switched on, the anode copper lost electrons and became Cu^{2+} dissolved in the solution, while the cathode Cu^{2+} gained electrons and was reduced to Cu atom. PEG on the surface of WC had a synergistic effect with Cl^- in the electroplating solution, and it chelated with copper ions to form a PEG– Cu^+ – Cl^- complex [30]. The complex produced a passivation film on the surface of WC, which likely inhibited the reduction rate of Cu ions during the electroplating process. SDS accelerates atomic deposition and is often used as a promoter. The acceleration is due to the molecular structure of SDS, including the head adsorption group that effectively adsorbs the copper plating layer and the terminal anionic group that adsorbs positively charged copper ions from the copper plating solution. Here, SDS was adsorbed on the surface of WC nanoparticles and attracted positively charged

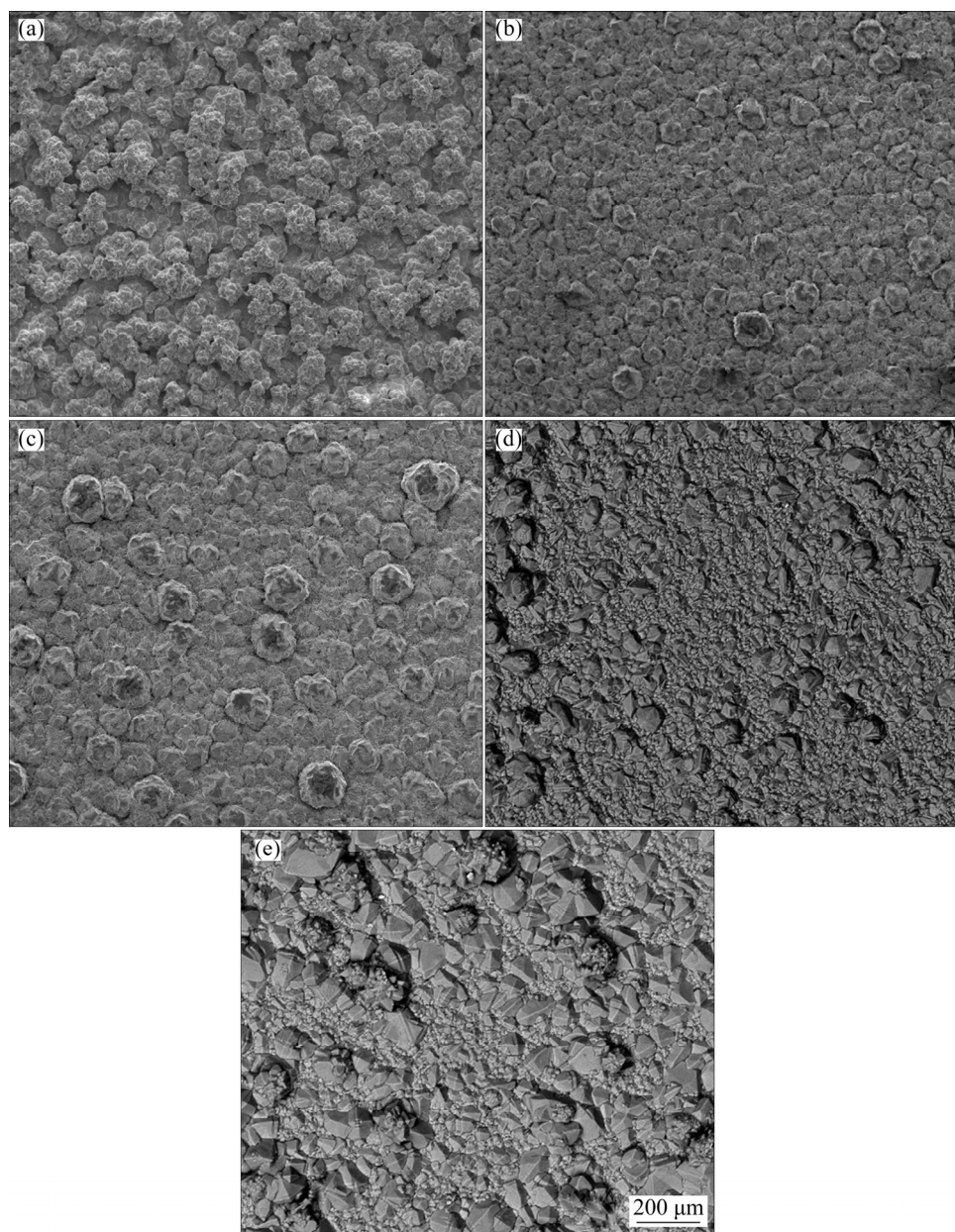


Fig. 8 SEM surface morphologies of WC–Cu composite: (a) Sample 1; (b) Sample 2; (c) Sample 3; (d) Sample 4; (e) Sample 5

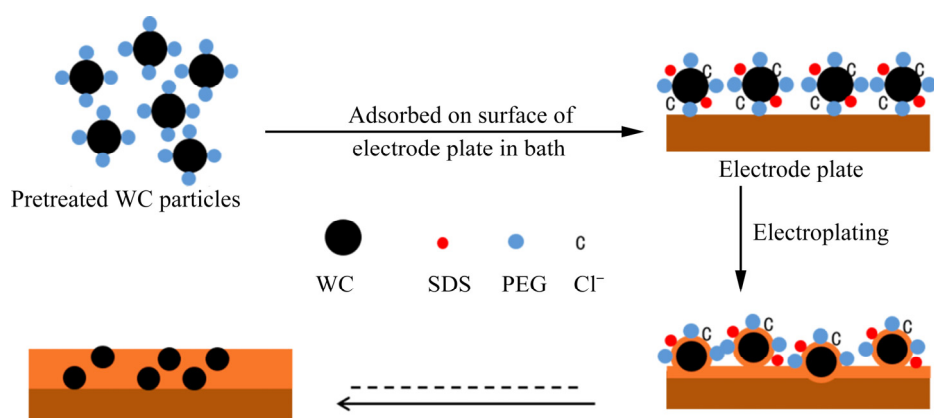


Fig. 9 Formation schematic of WC–Cu composites by electroplating

copper ions during electroplating. The synergistic effect of additives made the copper prepared by electroplating more compact, and caused the WC nanoparticles to be evenly dispersed in the copper matrix to form WC–Cu composite.

3.3 Properties of plating composites

Table 2 presents the relative density values of samples electroplated with different concentrations of WC and additives. The density of samples increased initially and then decreased with increase in amount of WC. This is consistent with the reduction of material shrinkage by the addition of WC particles. When the concentrations of PEG, SDS and WC were 0.2, 0.1 and 5 g/L, respectively, the relative density of the sample was as high as 85.6% without distortions. This is similar to the result of composite with equal WC content prepared by common sintering method, which is about 80% [31]. This is consistent with the analysis results in Fig. 5. Sample 3 has the least holes and the best compactness. Therefore, Sample 3 has the highest relative density.

Table 2 Relative density of samples electroplated with different concentrations of WC and additives

Sample No.	Relative density/%
1	73.8
2	77.8
3	85.6
4	72.9
5	69.5

The effects of WC and additives on the hardness of the WC–Cu composite compared with pure Cu are shown in Fig. 10. The hardness of WC–Cu composite increased with increase in WC content. The highest value for hardness of composite (Sample 4) was HV 221, which was 2.5 times that of pure copper. The high hardness of WC–Cu composite can be attributed to the effect of WC. However, the hardness decreased dramatically when the WC concentration was 15 g/L in Bath 5 (Sample 5), which was due to the pores in the sample. Also, the hardness of Sample 1 was lower than that of pure copper because the sample was not compact.

Figure 11 shows the electrical conductivity results of the WC–Cu composite. As expected, the

electrical conductivity of WC was much lower than that of copper, and the composite of the two materials can inevitably provide additional interfaces and increase electron scattering. The electrical conductivity of Sample 1 was 41.2 MS/m, which was significantly lower than that of Sample 2 and Sample 3. Although the content of WC in Samples 1, 2 and 3 was the same in the electroplating bath used in the preparation process, the number of pores in Sample 1 was larger than that in Sample 2, due to the different additives used (Fig. 5). These pores blocked the electron transmission, resulting in the lower electric conductivity. Sample 5 contained a large number of pores. Thus, the electrical conductivity of Sample 5 was the lowest, 39.6 MS/m. It is noteworthy that the conductivity of Samples 3 and 4 (55.6 and 53.7 MS/m, respectively) was not significantly lower compared to that of pure copper. The large deviation in the multiple conductivity measurements of Sample 1 and Sample 5 was possibly due to the uneven current conduction caused by the

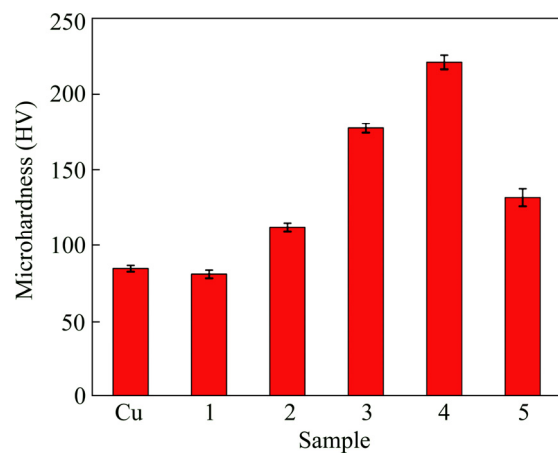


Fig. 10 Hardness of WC–Cu composites

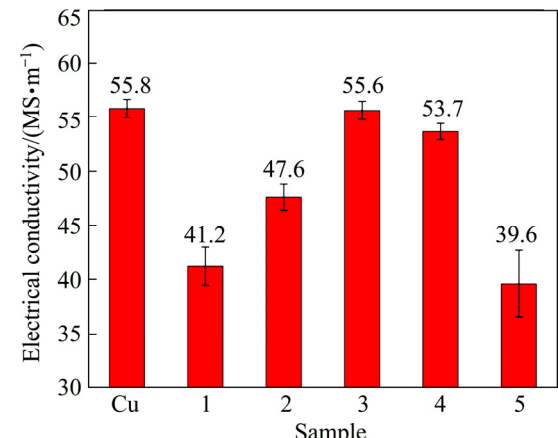


Fig. 11 Electrical conductivity of WC–Cu composites

increase of holes and WC content in the composite, which led to the increase in error of the measurement results.

Compared to the properties of WC–Cu composite prepared by traditional sintering methods, the WC–Cu composite prepared by electroplating exhibited higher hardness and better electrical conductivity. This may be due to the compact WC–Cu structure obtained by electroplating, which is conducive to electron propagation and flow.

4 Conclusions

(1) In the WC–Cu composite prepared, WC uniformly distributed in a copper matrix. WC–Cu composite was obtained with high hardness (HV 221) and high electrical conductivity (53.7 MS/m) when the electroplating bath consisted of 10 g/L of WC nanoparticles, 0.2 g/L of PEG and 0.1 g/L of SDS.

(2) The excessive addition of WC nanoparticles was found to obstruct the electroplating process, resulting in more holes and less compact layers.

(3) TEM results confirmed the existence of WC in the Cu matrix with tight binding of WC to Cu atoms.

(4) By adjusting the content of additives and WC nano powders, compact WC–Cu composite with excellent properties can be prepared by electroplating. This lays a good foundation for the application of such electrical contact materials widely used in automobiles, electronics, aerospace and other fields.

References

- [1] KELLY T G, CHEN J G G. Metal overlayer on metal carbide substrate: Unique bimetallic properties for catalysis and electrocatalysis [J]. Chemical Society Reviews, 2012, 41(24): 8021–8034.
- [2] COLTON R J, HUANG J T J, RABALAIS J W. Electronic structure of tungsten carbide and its catalytic behavior [J]. Chemical Physics Letters, 1975, 34(2): 337–339.
- [3] DESHPANDE P K, LIN R Y. Wear resistance of WC particle reinforced copper matrix composites and the effect of porosity [J]. Materials Science and Engineering A, 2006, 418: 137–145.
- [4] DIAS M, PINHAO N, FAUSTINO R, MARTINS R M S, RAMOS A S, VIEIRA M T, CORREIA J B, CAMACHO E, FERNANDES F M B, NUNES B, ALMEIDA F A, MARDOLCAR U V, ALVES E. New WC–Cu composites for the divertor in fusion reactors [J]. Journal of Nuclear Materials, 2019, 521: 31–37.
- [5] ABYZOV A M, KRUSZEWSKI M L A J, CIUPINSKI L U, MAZURKIEWICZ M, MICHALSKI A, KURZYD K J. Diamond–tungsten based coating–copper composites with high thermal conductivity produced by pulse plasma sintering [J]. Materials and Design, 2015, 76: 97–109.
- [6] YANG Xiao-hong, LIANG Shu-hua, WANG Xian-hui, XIAO Peng, FAN Zhi-kang. Effect of WC and CeO₂ on microstructure and properties of W–Cu electrical contact material [J]. International Journal of Refractory Metals and Hard Materials, 2010, 28: 305–311.
- [7] YAO Gong-cheng, CAO Che-zheng, PAN Shuai-hang, SOKOLUK M, LI Xiao-chun. High-performance copper reinforced with dispersed nanoparticles [J]. Journal of Materials Science, 2019, 54: 4423–4432.
- [8] CABEZAS-VILLA J L, OLMOS L, VERGARA-HERNÁNDEZ H J, JIMÉNEZ O, GARNICA P, BOUWARD D, FLORES M. Constrained sintering and wear properties of Cu–WC composite coatings [J]. Transactions of Nonferrous Metals Society of China, 2017, 27: 2214–2224.
- [9] WAN B Q, SUN X Y, FENG H T M R F, LI Y S, YANG Q. Plasma enhanced chemical vapor deposition of diamond coatings on [J]. Surface and Coatings Technology, 2015, 284: 133–138.
- [10] ZHAO Nai-qin, LI Guo-jun, WANG Chang-ju. Study on electric resistance welding electrode made with PM vacuum hot-pressed WC/Cu composite [J]. Ordnance Material Science and Engineering, 1997, 20(3): 39–44.
- [11] ZHANG Cheng-cheng, LUO Guo-qiang, ZHANG Jian, DAI Yang, SHEN Qiang, ZHANG Lian-meng. Synthesis and thermal conductivity improvement of W–Cu composites modified with WC interfacial layer [J]. Materials and Design, 2017, 127: 233–242.
- [12] SOLOVJEV D S, SOLOVJEVA I A, KONKINA V V, LITOYKA Y V. Improving the uniformity of the coating thickness distribution during electroplating treatment of products using multi anode baths [J]. Materials Today: Proceedings, 2019, 19: 1895–1898.
- [13] ANIJDAN S H M, SABZI M, ZADEH M R, FARZAM M. The effect of electroless bath parameters and heat treatment on the properties of Ni–P and Ni–P–Cu composite coatings [J]. Materials Research, 2018, 21(2): e20170973.
- [14] PULSFORD J, VENTURI F, PALA Z, KAMNIS S, HUSSAIN T. Application of HVOF WC–Co–Cr coatings on the internal surface of small cylinders: Effect of internal diameter on the wear resistance [J]. Wear, 2019, 432–433: 202965.
- [15] SABZI M, DEZFULI S M, MIRSAEEDGHAZI S M. The effect of pulse-reverse electroplating bath temperature on the wear/corrosion response of Ni–Co/tungsten carbide nanocomposite coating during layer deposition [J]. Ceramics International, 2018, 44(16): 19492–19504.
- [16] WU Zi-yi, ZHANG Jin-yong, SHI Tao-jie, ZHANG Fan, LEI Li-wen, XIAO Han, FU Zheng-yi. Fabrication of laminated TiB₂–B₄C/Cu–Ni composites by electroplating and spark plasma sintering [J]. Journal of Materials Science and Technology, 2017, 33(10): 1172–1176.

[17] ANIJDAN S H M, SABZI M, ZADEH M R, FARZAM M. The influence of pH, rotating speed and Cu content reinforcement nano-particles on wear/corrosion response of Ni–P–Cu nano-composite coatings [J]. *Tribology International*, 2018, 127: 108–121.

[18] BARRENA M I, GOMEZ de SALAZAR J M, MATESANZ L. Interfacial microstructure and mechanical strength of WC–Co/90MnCrV₈ cold work tool steel diffusion bonded joint with Cu/Ni electroplated interlayer [J]. *Materials and Design*, 2010, 31: 3389–3394.

[19] MERSAGH D S, SABZI M. Deposition of ceramic nanocomposite coatings by electroplating process: A review of layer-deposition mechanisms and effective parameters on the formation of the coating [J]. *Ceramics International*, 2019, 45(17): 21835–21842.

[20] ZHOU Ji-xue, ZHAO Guo-chen, LI Jin-shang, CHEN Jie, ZHANG Su-qing, WANG Jin, WALSH F C, WANG Shun-cai, XUE Yan-peng. Electroplating of non-fluorinated superhydrophobic Ni/WC/WS₂ composite coatings with high abrasive resistance [J]. *Applied Surface Science*, 2019, 487: 1329–1340.

[21] AKBULUT H, HATIPOGLU G, ALGUL H, TOKUR M, KARTAL M, UYSAL M, CETINKAYA T. Co-deposition of Cu/WC/graphene hybrid nanocomposites produced by electrophoretic deposition [J]. *Surface and Coatings Technology*, 2015, 284: 344–352.

[22] SABZI M, ANIJDAN S H M, ROGHANI Z M, FARZAM M. The effect of heat treatment on corrosion behavior of Ni–P–3 g/L Cu nano-composite coating [J]. *Canadian Metallurgical Quarterly*, 2018, 57(3): 350–357.

[23] YE Nan, TANG Jian-cheng, WU Ai-hua, WEI Xiao-xiao. Process and mechanism of WC nano-powders prepared by carbon-hydrogen coreduction-carbonization method [J]. *Rare Metal Materials and Engineering*, 2017, 46(1): 143–149. (in Chinese)

[24] LEE H, TSAI S T, WU P H, DOW W P, CHEN C M. Influence of additives on electroplated copper films and their solder joints [J]. *Materials Characterization*, 2019, 147: 57–63.

[25] LAI Zhi-qiang, WANG Shou-xu, WANG Chong, HONG Yan, ZHOU Guo-yun, CHEN Yuan-ming, HE Wei, PENG Yong-qiang, XIAO Ding-jun. A comparison of typical additives for copper electroplating based on theoretical computation [J]. *Computational Materials Science*, 2018, 147: 95–102.

[26] PENA E M D, ROY S. Electrodeposited copper using direct and pulse currents from electrolytes containing low concentration of additives [J]. *Surface and Coatings Technology*, 2018, 339: 101–110.

[27] ZHONG Huan, OUYANG Yue-jun, YU Gang, HU Bo-nian, YAN Da-long. Preparation of core-shell structured cobalt coated tungsten carbide composite powders by intermittent electrodeposition [J]. *Journal of Materials Science and Technology*, 2016, 32: 1171–1178.

[28] BRONGERSMA S, KERR E, VERVOORT I, SAERENS A, MAEX K. Grain growth, stress, and impurities in electroplated copper [J]. *Journal of Materials Research*, 2002, 17: 582–589.

[29] WATANABE T. Nano-plating microstructure formation theory of plated films and a database of plated films [M]. New York: Elsevier, 2004.

[30] LEE H, YU T Y, CHENG H K, LIU K C, CHAN P F, DOW W P, CHEN C M. Impurity incorporation in the Cu electrodeposit and its effects on the microstructural evolution of the Sn/Cu solder joints [J]. *Journal of the Electrochemical Society*, 2017, 164: 457–462.

[31] KELLY J J, TIAN C, WEST A C. Leveling and microstructural effects of additives for copper electrodeposition [J]. *Journal of the Electrochemical Society*, 1999, 146: 2540–2545.

添加剂及纳米 WC 粉含量对电镀 WC–Cu 复合材料性能的影响

赵玉超¹, 唐建成¹, 叶楠¹, 周威威¹, 韦朝龙¹, 刘定军²

1. 南昌大学 材料科学与工程学院, 南昌 330031; 2. 南昌大学 高等研究院, 南昌 330031

摘要: 研究添加剂(聚乙二醇(PEG)、十二烷基硫酸钠(SDS))和纳米 WC 粉对 WC–Cu 复合材料显微结构、相对密度、硬度和导电性的影响, 并对电镀制备机理进行研究。采用 XRD、SEM、EDS、TEM、HRTEM 等测试方法分析样品的显微结构。PEG 与 SDS 的协同作用使 WC–Cu 复合材料在电镀过程中更加致密。WC–Cu 复合材料的硬度随着 WC 含量的增加而增加, 导电性随 WC 含量的增加而降低。随着添加剂含量的增加, 样品的密度呈现先增大后减小的趋势。当电镀液中含有 10 g/L WC 纳米粉、0.2 g/L PEG 和 0.1 g/L SDS 时, WC–Cu 复合材料硬度为 HV 221、电导率为 53.7 MS/m。结果表明, 通过优化添加剂和纳米 WC 颗粒的含量, 可以得到性能优良的 WC–Cu 复合材料。

关键词: WC–Cu 复合材料; 电镀; 添加剂; 显微结构; 性能

(Edited by Bing YANG)